Indoor High-Bandwidth Optical Wireless Links for Sensor Networks

Jarir Fadlullah, *Student Member, IEEE*, and Mohsen Kavehrad, *Fellow, IEEE*

***Abstract*—Emergence of sensor networks for data-procurement in wide-ranging applications, including defense, medical, environmental and structural health monitoring, has led to development of low-power miniature devices employing radio frequency (RF) communications. In contrast to RF, optical devices are smaller and consume less power; reflection, diffraction, and scattering from aerosols help distribute signal over large areas; and optical wireless provides freedom from interference and eavesdropping within an opaque enclosure. Optics can accommodate high-bandwidth transmission of multimedia in aircrafts, where RF is shunned due to interference with control signals. These motivate use of optical wireless as a mode of communication in sensor networks. We have set up and experimented on an infrared laser transceiver test-bed with ceiling used as reflector to establish an intensity-modulated/direct-detected (IM/DD) link. Frequency measurements are conducted to characterize the link up to 1 GHz, and are transformed to obtain impulse responses and eye diagrams. These experimental findings demonstrate the capability of indoor optical wireless links of delivering 1 gigabit per second and beyond, without intersymbol interference. Thus, a broadband infrastructure can be deployed allowing high-quality audio-visual data communication among sensor nodes.**

***Index Terms*—Channel characterization, infrared, optical wireless communication, quasi-diffuse, sensor neworks.**

I. Introduction

SENSOR networks have recently emerged as a viable means of surveying and monitoring remote or inaccessible regions of interest in environments such as industrial plants, medical facilities, battlegrounds, climate observation, etc. A large number of miniaturized devices are deployed, usually in a random fashion, to procure information about temperature, pressure, chemical constituency, motion, etc. within the region. These sensor nodes need to communicate wirelessly in an *ad hoc* manner among themselves, and sometimes to a central control mechanism, which is responsible for controlling the environment and alerting. The communication mode traditionally has been radio frequency (RF) channels, as evident in the immense amount of published literature on wireless sensor networks. While RF communications allow propagation of signals over a large area, this suffers from several drawbacks. The most serious problem with using RF is interference among signals transmitted from sensors that are closely located, and interference with RF control signals in a plant or a vehicle. Furthermore, RF bandwidth is seriously constrained and regulated worldwide, and prone to eavesdropping unless some means of encryption is employed.

In this paper, we present an alternative communications mode for wireless sensor networks using infrared light. Optical communications has already found its place in moderate-distance free-space optical (FSO) links, indoor inter-device connectivity, and in indoor local area networks. However, the potential of optical links in wireless sensor networks has remained significantly unexplored, except in some published literature [1]–[3]. Optical communications has a number of features which are useful in the context of sensor networks, the first and foremost being the exclusivity from RF control signals in sensitive systems, such as aircraft control and monitoring. Due to short wavelengths, optical devices can be manufactured in small sizes, instead of requiring larger arrays that are prevalent in RF communications. Security is inherently included in the physical layer, since the light used to communicate among sensors is contained in the room or space where it is intended to be deployed. Furthermore, the spectral region corresponding to optical wavelengths is unregulated worldwide, allowing a reuse principle as in cellular communications.

However, there are challenges to be overcome when using infrared light for sensor communications. The optical signal has to be contained within the field-of-view (FOV) of the transmitter and receiver, and due to the random nature of deployment of sensors, this cannot be always fully ensured. Bandwidth reduces in non-line-of-sight (NLOS) links, due to multipath propagation. Increasing the FOV of the transceiver system, on the other hand, implies increase in transmit power to maintain a viable link and also increase in the interference plus noise floor for neighboring communicators. The phenomenon of multiple scattering can be taken advantage of by using certain wavelengths of light, i.e., ultraviolet range as suggested in [1], that have a large atmospheric backscatter coefficient enabling the light to reflect off of particles and dust suspended in air and reach the receiver with substantial intensity. Multispot diffuse configuration, first introduced in [4], appears to be a very robust setup to combat the problem of 'finding the spot' in the case of distributed sensors. As a whole, there is significant potential for optical wireless in sensor networks and this can lead to a transformational change in sensor networks in terms of available bandwidth, security, and interference mitigation. This area requires further research in terms of optimization and application-specific design.

The rest of this paper is organized as follows: Section II presents a brief discussion of previous research conducted on indoor optical wireless channels for communications purposes

Manuscript received April 13, 2010; revised August 16, 2010; accepted September 04, 2010. Date of publication September 16, 2010; date of current version October 20, 2010. This work was supported in part by the National Science Foundation (NSF) Electrical, Communications and Cyber Systems directorate under Award #824052 project "Broadband Sensors Optical Wireless Local Area Networks."

The authors are with the Department of Electrical Engineering, The Pennsylvania State University, University Park, PA 16802 USA (e-mail: jmf414@psu.edu; mkavehrad@psu.edu).

Digital Object Identifier 10.1109/JLT.2010.2076775

and for sensor networks; Section III outlines the measurement technique undertaken by the authors to obtain frequency and time domain characteristics of the channel; performance evaluation from measurement results, including delay spread, and eye diagrams are illustrated in Section IV; Section V concludes the paper with comments on the results and discussion on future work.

II. Background

Optical wireless communications in indoor environment was introduced as early as three decades ago [5]. Since then, channel measurement in different transmit-receive configurations has been conducted to obtain frequency domain characteristics in different bandwidth ranges [6]–[9]. Furthermore, simulation models are also available for indoor optical wireless channels [10], [11], and can be readily extended to investigate performance under the sensor networks paradigm. Several standard bodies such as IrDA and IEEE 802.11 have recognized line-of-sight light propagation as a viable physical layer (PHY) technology for data transmission [12], [13]; however, communication using diffusely scattered (visible) light is being discussed in the standards only recently with the formation of IEEE 802.15.7 Task Group on Wireless Personal Area Network (WPAN) [14]. Until now, frequency response measurements for non-line-of-sight diffuse links are available upto a bandwidth of 1 GHz [15], which clearly indicates the huge bandwidth available in the optical regime. However, these works have been in the context of indoor wireless communications, and many of the stated solutions would not be compatible in a sensor network framework. For example, [15] mentions the use of photomultiplier tubes (PMT) as the receiving element. While being highly sensitive in low light, PMTs demonstrate a sensitivity deterioration in the presence of high ambient light intensity. Furthermore, PMTs have a bigger size as compared to solid state devices, e.g., p-i-n photodiode and avalanche photodiode (APD). As a result, APDs may be preferred over PMTs for sensor networks applications.

So far, there have been few published articles that discuss optical wireless communications in the context of sensor networks. Some interesting in-depth analysis of optical links that utilize "solar-blind" ultraviolet light can be found in [1], [2]. Backscattering phenomenon, while being detrimental to line-of-sight communication links such as in FSO, can be used to the advantage of sensor networks for *ad hoc* communications between nodes with no line of sight. Ultraviolet light is suggested in [1], since this region of spectrum contains negligible amount of background solar radiation. To integrate optical links on miniaturized sensor devices, simple modulation and detection schemes, e.g., intensity-modulation/direct-detection (IM/DD), are preferred over more complex transmission methods. A laboratory experiment on optical wireless sensor network in multi-scattering channel is presented in [2], which deals with non-alignment issues and multi-access interference in the network environment. A method of reconfiguring network layer topology is discussed in [3].

In principle, the main challenge for optical wireless to be used in a sensor network is power and bandwidth degradation due to shadowing, non-alignment, diffusion and multi-scattering. In this paper, we also suggest an alternative transmission technique, namely spot-diffusing [4], which is able to distribute the signal over a large area without significant degradation.

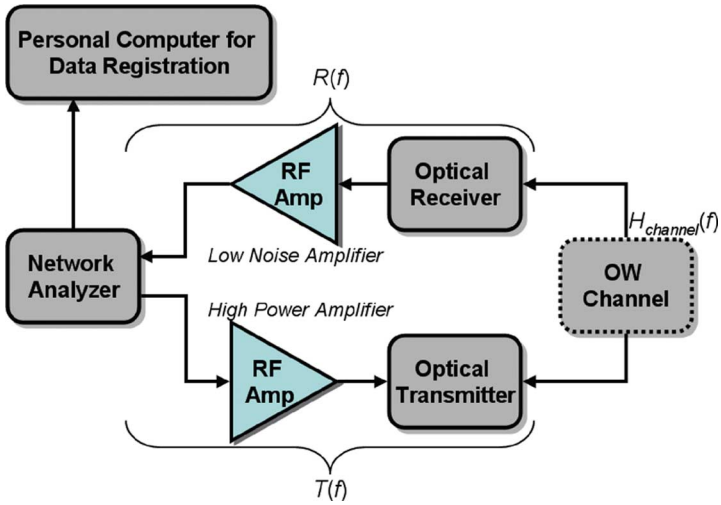

Fig. 1. Block diagram of the indoor optical wireless channel measurement setup.

III. Optical Indoor Wireless Channel Measurement

At present, there are high-bandwidth laser transmitters available in the market or can be built with off-the-shelf components, which can be coupled with high-gain and high-sensitivity photo-detectors, such as the photo-multiplier tube (PMT) and the avalanche photo-diode (APD). For example, frequency characterization with narrow FOV receivers has been conducted up to 1 GHz using laser diodes and PMTs in recent times [15]. In our measurements, we use a laser diode as the transmitter and an avalanche photodiode (APD) as the receiver, and obtain frequency domain responses.

A. Measurement Setup

The measurement system is comprised of a network analyzer, the Agilent ENA 5071C, which uses a CW swept frequency approach [6] to obtain the amplitude and phase characteristics of the channel at frequencies between 10 MHz and 1 GHz. Fig. 1 shows a block diagram of the indoor optical channel measurement system. The sinusoidal signal from the network analyzer is amplified using a HP 83006A high-power amplifier with a gain of 26 dB, before input to the laser transmitter. This ensures sufficient modulation depth of the transmit laser. An aspheric lens attached on the laser diode (JDS 2455-G1) produces a focused spot on the ceiling. The laser temperature is stabilized at room temperature with a Thorlabs TED350 temperature controller, and a Thorlabs LDC240C current controller. For the receiver, an avalanche photo-diode, APD210 from Menlo Systems with an integrated adjustable-gain low-noise amplifier, is chosen for its high-sensitivity, and high gain, as opposed to previous high-frequency measurements [15]. Due to the small APD sensitive area, it is very difficult to detect any signal at a distance without a lens assembly. Therefore, a focusing lens is attached to the photodetector to collect sufficient reflected light and focus it on the active detector area. When a 2-inch diameter lens is

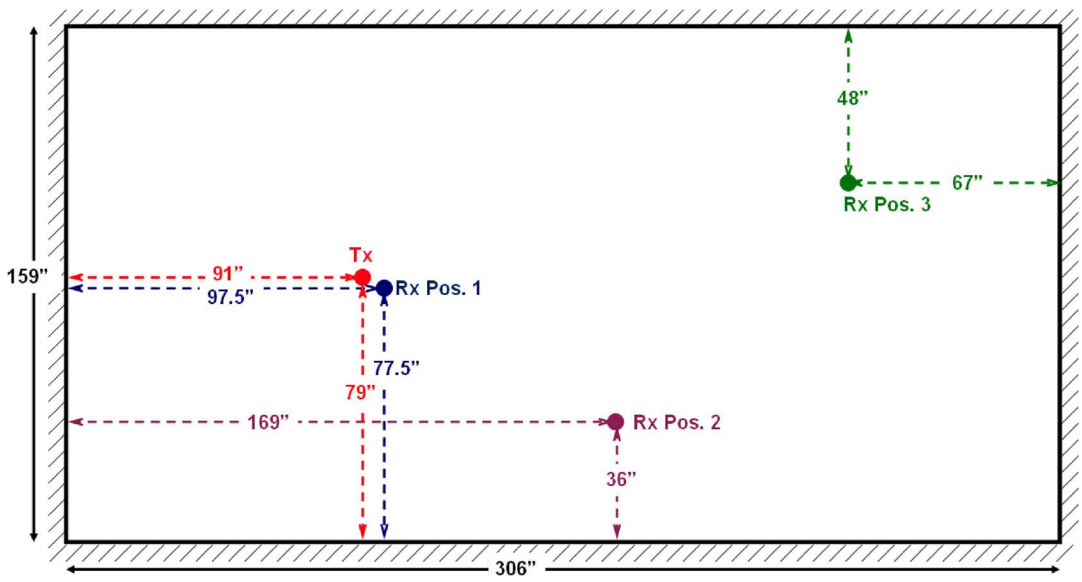

Fig. 2. Room layout showing relative positions of the optical transmitter and receiver.

used, the ratio of receiving lens area to the detector area is approximately 10 000. This provides about 40 dB power enhancement to overcome path loss due to propagation. The output of the receiver is fed to a low-noise amplifier, which is connected to the measurement port of the network analyzer using a shielded coax cable. A ratio measurement is done with respect to the reference transmitted signal to find out the amplitude and phase responses over the bandwidth of interest.

Transmitted power level is set at 50 mW, which is sufficiently low so as not to saturate the APD. This quantity may not be eye-safe when looked directly towards the laser source; however, the collimated light is diffused at the ceiling yielding an irradiance of 159 μW/cm^2 at 0.1 m distance, which is much lower than the 8.37 mW/cm^2 hazard limit (calculated in Section IV.D) specified for 808 nm light by the IEC 60825-1 Laser Safety Standard [16]. While the focusing lens assembly is useful to collect sufficient power, it renders the transmit and the receive optics sensitive to appropriate alignment. To align them properly, the receiver is mounted on a rotary assembly with gimbals, which enables it to be rotated and pointed toward any direction, and as such can be moved to any other location inside the room for measurement.

The laser is modulated in the specified frequency range by the network analyzer using a Bias-Tee network included in the laser mount. To ensure operation in the linear regime, RF power output of the network analyzer is set to 0 dBm. This generated a modulating current swing of 6.32 mA, giving a minimum laser current of about 360 mA, which is well above the specified laser threshold current of 320 mA. The received power at the APD was also below the maximum incident power rating of 10 mW, and its gain was set properly to ensure linear operation.

Measurements are carried out at three different locations in a standard laboratory room, as shown in Fig. 2, with lenses of three different diameters: 1″, 2″, and 3″. The room is about 7.8 meters (306 inches) long by 4 meters (159 inches) wide. The room ceiling is about 2.5 meters (100 inches) above the laser transmitter and receiver. The dimensions of the room and the relative locations of the transmitter and the receiver are shown in Fig. 2. For each measurement, the transmitter is kept fixed at one location, while the receiver setup is moved from one location to another. The room is darkened during measurements to reject interference from ambient light, although the fluorescent lighting is observed to have no appreciable effect on the measured responses. The measurement parameters are summarized in Table I.

TABLE I
INDOOR OPTICAL WIRELESS FREQUENCY DOMAIN MEASUREMENT PARAMETERS

Parameter	Value
Number of Points	1601
Frequency Range	10MHz–1GHz
IF BW	10 Hz
Operating Wavelength	808nm
Average optical output power of laser diode	50mW
Detector active area	0.1963mm^2
Detector rise time	0.5ns
Focal length of receiving lens	35mm (1") 75mm (2") 85mm (3")
Receiving lens area	5.07cm^2 (1") 20.27cm^2 (2") 45.6cm^2 (3")

This setup is effectively an indoor directed non-line-of-sight configuration [17], where the transmitter sends modulated collimated light towards the ceiling, which acts as a secondary Lambertian (diffuse) source, and the reflected signal is captured at

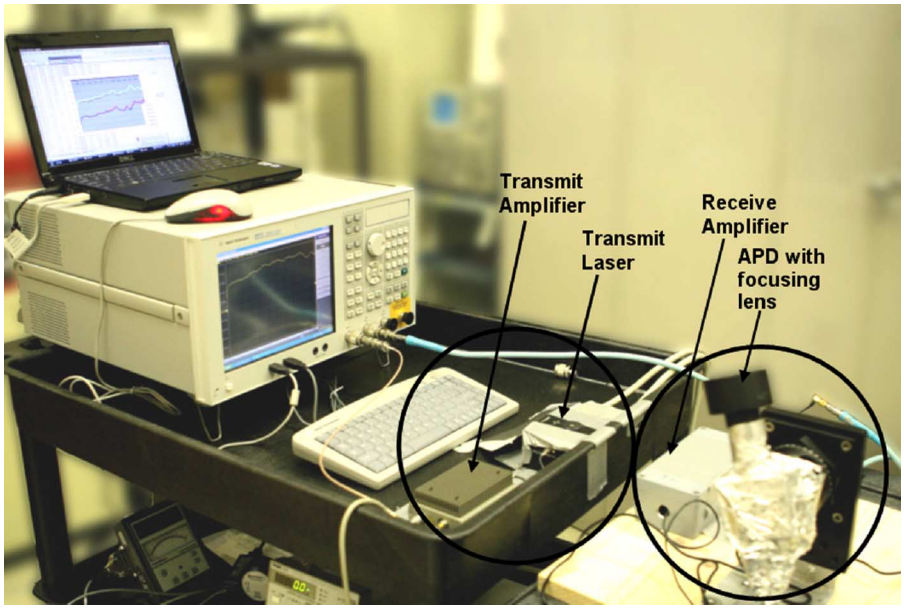

Fig. 3. Photograph of experimental setup.

the receiver through a focusing lens, which is pointed towards the ceiling spot. Fig. 3 shows the experimental setup.

B. Calibration of Results

To obtain the channel characteristics, the responses of the optical transmitter, receiver and amplifiers have to be subtracted from the data obtained from the measurement described in Section III.A. This requires the laser transmitter and the APD to be placed back-to-back [7], with the channel excluded. To protect the APD from exceeding exposure, the laser power is attenuated to a controlled level by covering with a thick black paper with a pinhole. As a result, the channel is replaced with a constant attenuation factor, which is found by measuring the unobstructed laser power and the power at the pinhole with an optical power sensor. The measured back-to-back frequency response is then given by

$$H_{\mathrm{ref}}(f) = T(f) \cdot K_{\mathrm{att}} \cdot R(f) \tag{1}$$

where transmitter side frequency response is $T(f)$, the receiver side response is $R(f)$, and K_{att} is a frequency-independent attenuation constant.

When the measurement is done with the propagation channel between the transmitter and the receiver, we obtain the non-calibrated channel response as

$$H(f) = T(f) \cdot H_{\mathrm{channel}}(f) \cdot R(f). \tag{2}$$

To obtain the calibrated channel response, (2) is divided by (1) and multiplied by the known attenuation constant, K_{att}, which gives

$$H_{\mathrm{channel}}(f) = H(f) \cdot K_{\mathrm{att}} / H_{\mathrm{ref}}(f). \tag{3}$$

This quantity corresponds to the frequency response of the channel under consideration.

C. Frequency Domain Results

At the locations shown in Fig. 2, frequency response measurements are conducted from 10 MHz in steps of 618.75 kHz to 1 GHz, giving a set of 1601 uniformly spaced points in frequency for each measurement. Since the frequency response is characterized up to 1 GHz, the resolution of the impulse response obtained by Fourier transform would be $1/(2\times 10^9) = 0.5$ ns. Due to the DC-blocking capacitive effects of the amplifying section of the receiver, the start frequency is chosen as high as 10 MHz. The intermediate frequency (IF) bandwidth of the network analyzer was set to 10 Hz to reduce the fluctuations in the data registered on the network analyzer. Magnitude and phase responses, calibrated according to the method described in Section III.B, are illustrated in Fig. 4, for the three different lens assemblies and the three different locations shown in Fig. 2. In our measurements, the receiving lens forms part of the channel, and thus is included in the channel frequency and impulse responses.

Fig. 4 demonstrates that the measured magnitude responses are almost flat over the entire bandwidth of interest, and furthermore, the phase responses are linear over that range. With change in location, the responses retain their shapes and attenuate by a constant amount, due to increased path loss or increased distance from the transmitter. On the other hand, the lens with the largest collecting surface experiences the least attenuation, irrespective of location.

The flatness of the frequency response is due to having only the line-of-sight component of the reflected light impinging on the receiving aperture. Therefore, no multiple-bounce reflection components should appear in the impulse response, and it would ideally consist of a finite impulse located at the delay corresponding to propagation distance. The magnitude also corresponds to the amount of optical power collected by the receiving optics with an ideal Lambertian source located at the ceiling spot.

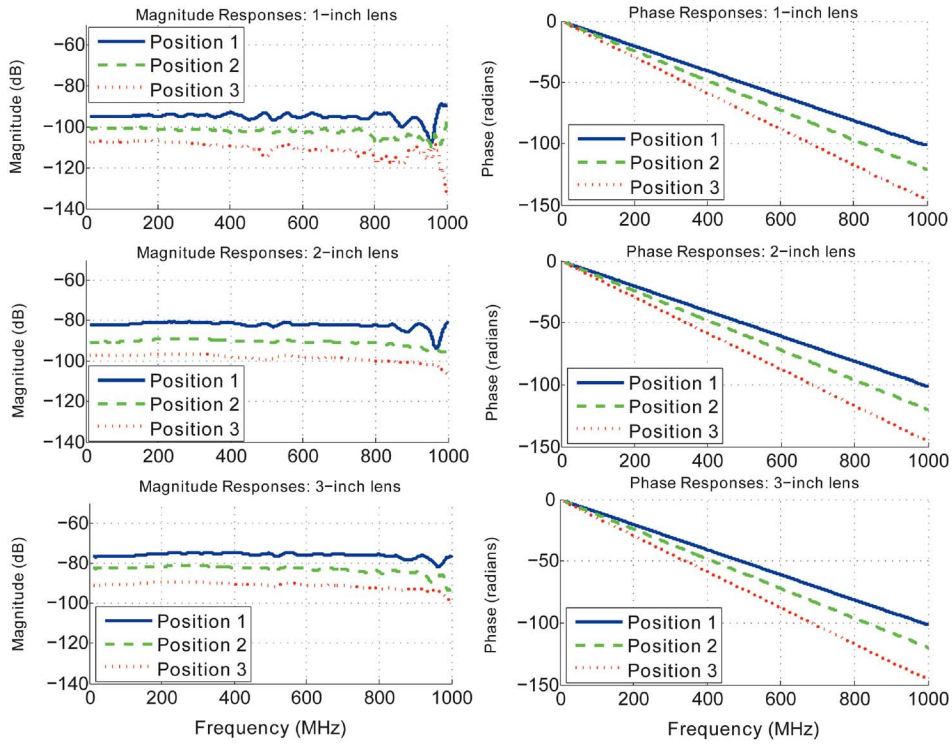

Fig. 4. Measured and calibrated magnitude and phase responses.

D. Time Domain Analysis

To better understand the effect of the channel on a high-speed transmission link, the electrical-domain impulse response is required. This is obtained by appropriately Fourier-transforming the frequency responses obtained in Section III.C. Since the transfer ratios for DC and near-DC frequencies are absent, frequency measurements are extended to DC by interpolation. Savitzky-Golay filtering is applied on the frequency response to smoothen it and to reduce effects of noise, in a manner similar to [6]. Furthermore, windowing is applied to the responses before taking the inverse Fourier transform, which helps reduce sidelobe levels in the impulse response. Several different windowing functions have been used in previous works, including Hamming [9] and Blackman [15]. We choose the Kaiser window, since this has been established as a *de facto* standard for network analyzers which have impulse response transformation and display capability [18]. The Kaiser window is given by

$$w_n = \begin{cases} \dfrac{I_0\left(\pi\alpha\sqrt{1-\left(\frac{2n}{M}-1\right)^2}\right)}{I_0(\pi\alpha)} & 0 \le n \le M, \\ 0 & \text{otherwise.} \end{cases} \tag{4}$$

The reason for selecting the Kaiser window is its near-optimal maximum energy concentration near low frequencies, as required for response estimation from finite length segments of data [19]. The frequency span of the measurements, as well as the roll-off (α) factor, affects the sidelobe levels and the 3-dB impulse width of the windowing function. Therefore, the desired temporal resolution of the impulse response must be taken into account before choosing α. The approximate impulse width of Kaiser window with α parameters $\{0, 6, 13\}$ is $\{0.6, 0.98, 1.39\}$ divided by the frequency span of the two-sided response [18]. We chose the α parameter of our Kaiser window to be 6, giving an impulse width of $0.98/2 \times 10^9$ or 0.49 ns, which is less than the 0.5 ns temporal resolution imposed by the APD rise-time limitation. The sidelobe attenuation level of the selected window is as low as -44 dB with respect to the main lobe [18]. This ensures proper sidelobe level reduction, while maintaining desired temporal resolution.

The resulting impulse responses for the three lens assemblies at the three locations are shown in Fig. 5. These are truncated at 50 ns, which is the propagation delay corresponding to about twice the length of the room. This limits only the direct reflection and first reflections from walls to appear in the impulse response. The impulse responses are positive and their peak values occur at a delay consistent with the propagation distance. The ideal impulsive nature is not seen due to the finite resolution of the measurement system; however, as surmised previously, there are no multiple-bounce components in the impulse response. On a contrary note, having a diffuser in front of the laser transmitter and having a wider field-of-view at the receiver would have created strong multipath components, and would widen the tail of the impulse responses. This would also require more power to sustain a viable communication link.

The impulse responses illustrated in Fig. 5 form the basis of the performance evaluation presented in the next section.

IV. Performance Evaluation

In this section, the data rate performance of the optical wireless link is evalulated from the response characteristics obtained in Section III, in terms of delay spread and eye diagrams.

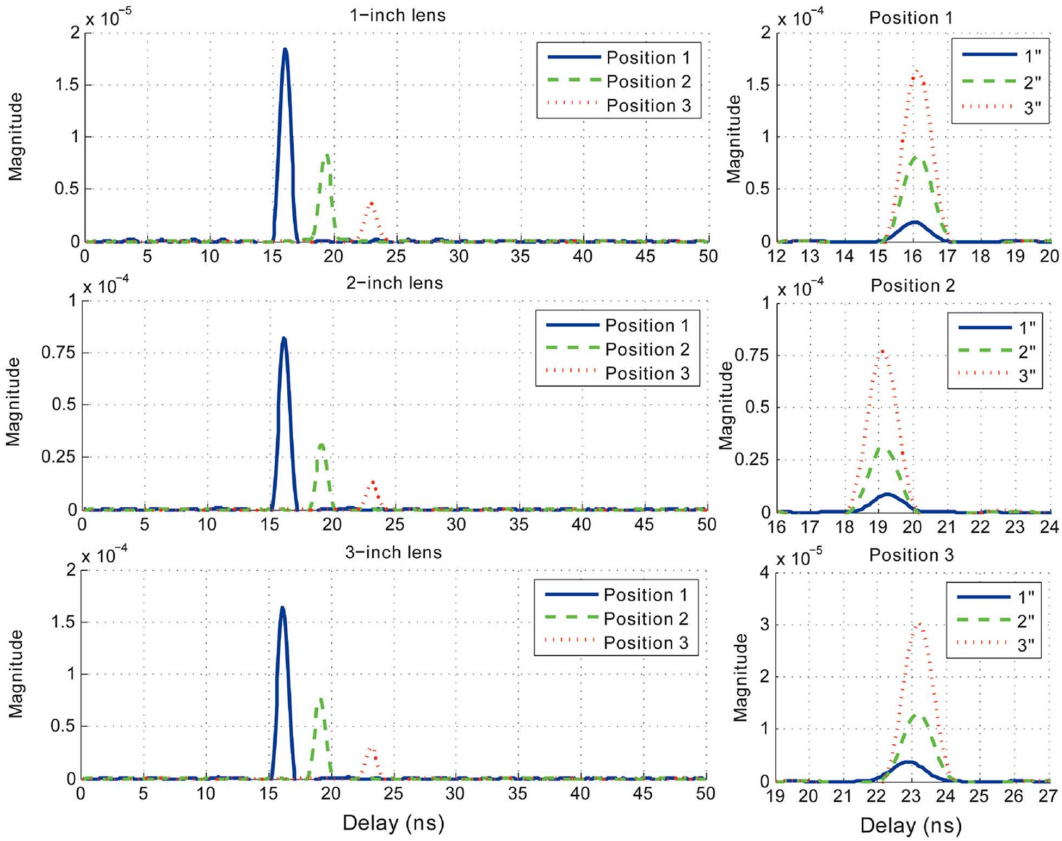

Fig. 5. Impulse responses obtained through inverse Fourier transform of measured frequency responses.

TABLE II
DELAY SPREAD (σ_τ) VALUES FOR MEASUREMENT LOCATIONS

	Position 1	**Position 2**	**Position 3**
1-inch lens	0.4268ns	0.3482ns	0.4105ns
2-inch lens	0.3419ns	0.3317ns	0.3400ns
3-inch lens	0.3278ns	0.3264ns	0.3376ns

A. Delay Spread Calculation

Delay spreads give an initial estimate of the data rate performance of the channel and can be computed from impulse responses. The average delay, μ_τ, and the rms delay spread, σ_τ, are given by [7]

$$\mu_\tau = \frac{\int_0^\infty t h^2(t)dt}{\int_0^\infty h^2(t)dt} \tag{5}$$

$$\sigma_\tau = \sqrt{\frac{\int_0^\infty (t-\mu_\tau)^2 h^2(t)dt}{\int_0^\infty h^2(t)dt.}} \tag{6}$$

Delay spread values calculated, using (5) and (6), from the impulse responses shown in Fig. 5, and tabulated in Table II.

From Table II, the root-mean-square delay spread values for all three lenses at the three locations are seen to be close to 0.5 ns. This is because the measurement of the channel is limited by the devices themselves, and not by the channel. For a realistic scenario, we can approximate the delay spread to 0.5 ns, taking the device limitation as the channel limitation. The inverse of the delay spread is proportional to the coherence bandwidth, which is the bandwidth over which the channel can be considered "flat", i.e., the frequencies within this band experience similar amount of attenuation, and as a result, there should be no intersymbol interference in time domain. If the true delay spread value is taken to be on the order of the measurement resolution, the coherence bandwidth would be $1/(0.5\times10^{-9}) = 2$ GHz. On a first approximation basis, this means that the wireless optical link under measurement can support data rates well beyond 1 Gbps, without requiring complex equalization schemes as are necessary for RF wireless and most wireline communication media.

B. Performance in Noise

Delay spread calculation, however, does not reflect the performance of the optical wireless system in additive noise and background radiation. To examine the effects of noise on a high-speed data transmission link using optical wireless, we calculate the variance of the background light-induced shot noise component in the output current as $\sigma_{bn}^2 = 2{\cdot}q{\cdot}P_{bn}{\cdot}A_R{\cdot}\Delta\lambda{\cdot}R{\cdot}B$, where q is one electron charge, P_{bn} is the background optical intensity, A_R is receiver area, $\Delta\lambda$ is the width of the optical filter, R is detector responsivity, and B is the bit rate of the communication system [20], [21]. The noise variance in the preamplifier stage of the receiver is given by $\sigma_{pr} = (\mathrm{NEP})\cdot\sqrt{B}$, where NEP is the noise-equivalent power of the detector. In accordance with [22], we assume, $P_{bn} = 6$ μW/(cm^2·nm), and $\Delta\lambda = 30$ nm; R

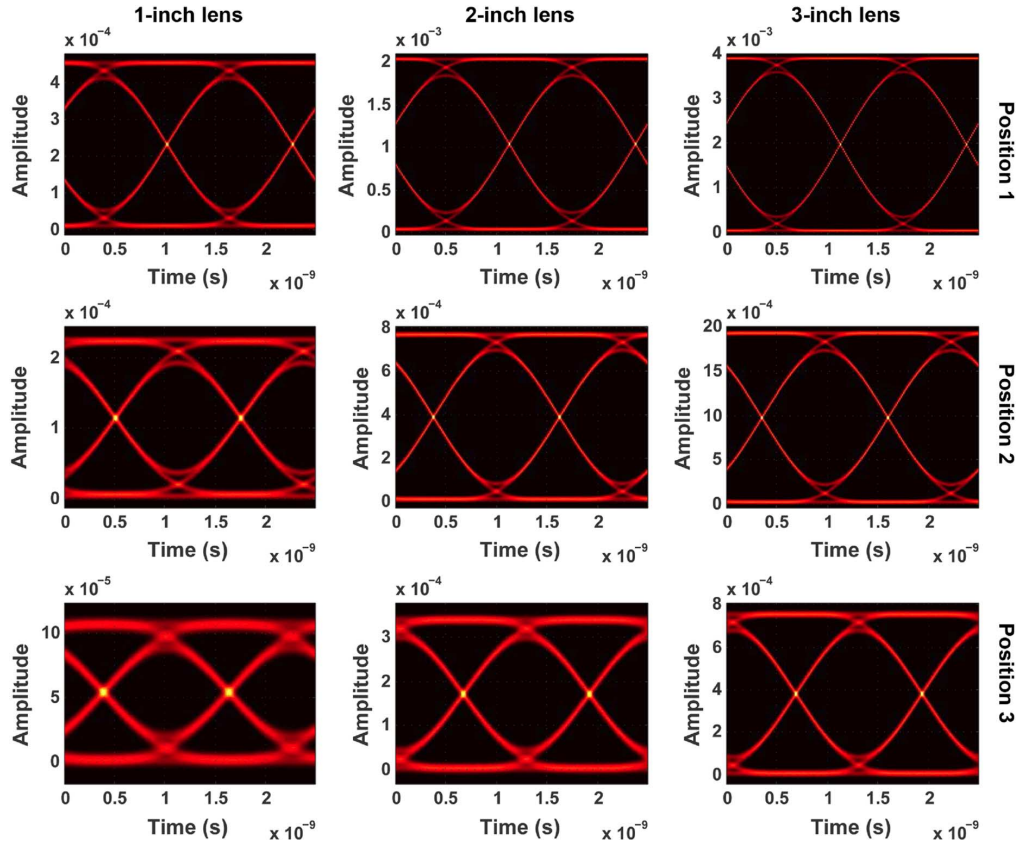

Fig. 6. Eye Diagrams at 800 Mbps data rate.

is 50 A/W and NEP is 0.4 pW/$\sqrt{\text{Hz}}$ according to specifications, and B is 10^9 for 1 Gbps and 8×10^8 for 800 Mbps transmission.

With these quantities, the total variance of the additive noise is computed, and used to evaluate the eye diagrams with the impulse responses obtained in Section III.D.

C. Eye Diagrams

Using the impulse response obtained in Section III.D, simulations were run for a 1 Gbps and 800 Mbps indoor optical wireless links with the receiver located at the three different positions. The modulation technique was chosen to be On-Off Keying (OOK) modulation, since OOK is the most widely used transmission scheme for such links, and offers least complexity of implementation without unreasonable degradation in performance. The pulses transmitted from the laser are rectangular with maximum power output occuring during symbol '1' and no power is output during symbol '0'. The average transmit power of the modulated data stream is also changed to use the complete linear range within which the laser can be modulated. Thus, the average optical power output of the laser can be increased to 24.7 dBm. This power does not exceed eye-safety limitations as discussed in Section IV.D, and the chosen laser is capable of providing linear modulation in this range. The additive noise was assumed Gaussian with variance computed from Section IV.B. The resulting eye diagrams are illustrated in Figs. 6 and 7 for 800 Mbps and 1 Gbps data rates, respectively. Pseudo-random binary sequences of 100 000 bits are used to generate these eye diagrams, which show two consecutive bit intervals in each plot.

The eye diagrams consistently show that the "open-eye" condition is satisfied for the three lenses at all three locations inside the room. The noise and background interference becomes more and more prominent in longer propagation distances, furthermore the larger lenses collect more background interference than the smaller lenses. For 800 Mbps, the eye diagrams are found to be almost ideal with little overlap between consecutive symbols, whereas there is some visible overlap between symbols for 1 Gbps, which results from the window function not being able to apply sufficient attenuation near the tail of the impulse response at this high rate. The eyes are still observed to be sufficiently open and binary detection can be applied with slightly degraded performance. In general, it can be concluded from the eye diagrams that transmission of at least 1 Gbps data is feasible through an indoor optical wireless channel.

D. Eye Safety Considerations

The wavelength chosen here for measurement and performance evaluation is 808 nm, and is therefore subject to exposure limitation for eye and skin safety [16]. The maximum permissible exposure (MPE) for the wavelength under consideration can be calculated from Clause 13.3 of the IEC 60825-1 standard, and is the minimum of three restrictive requirements. To get the minimum safe level, we assume direct ocular viewing (correction factor $\mathrm{C}_4 = 1$), and exposure time limited by blink reflex (0.25 s). Correction factor C_6 is calculated to be 1.6444, single pulse duration is 10^{-9} s, and the average number of pulses in the exposure time is 1.25×10^8. With these quantities, requirement

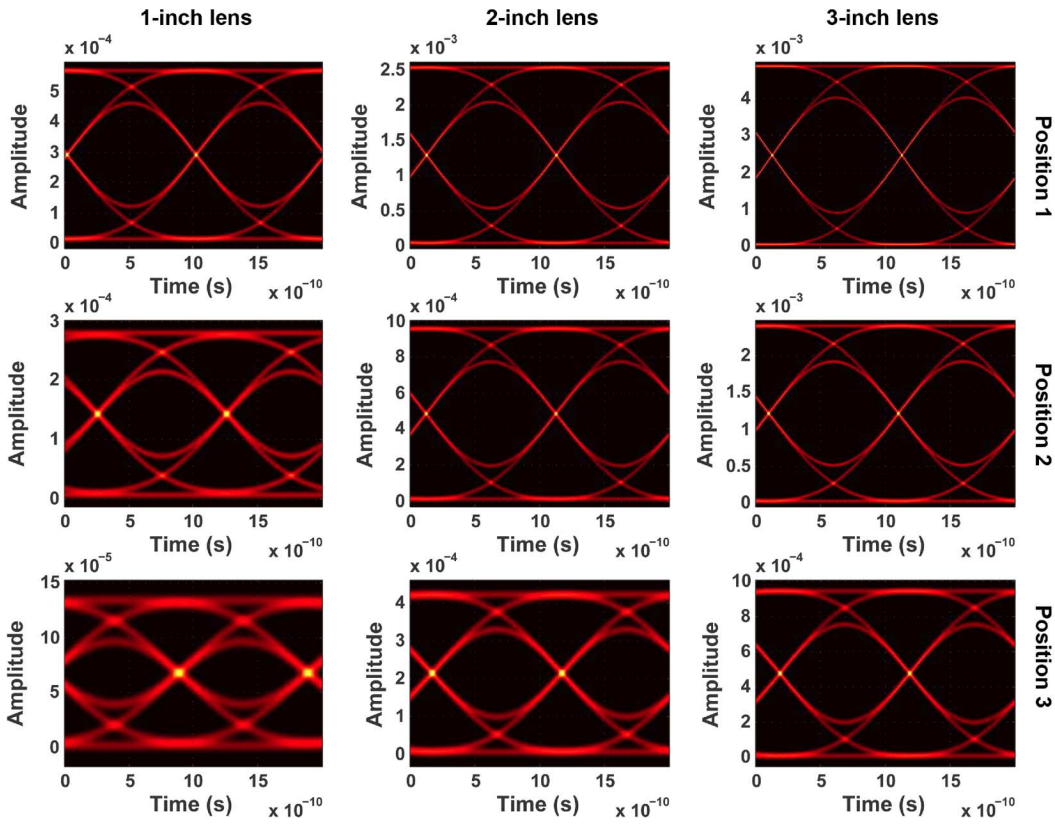

Fig. 7. Eye Diagrams at 1 Gbps data rate.

13.3(a) of [16] yields a MPE of 8.222×10^2 W/cm^2, whereas 13.3(b) and 13.3(c) give 8.37 mW/cm^2 and 7.78 W/cm^2. Therefore, the MPE is 8.37 mW/cm^2. For the hypothetical data transmission system described in this section, a single transmitted pulse from the ceiling diffusing spot would have an irradiance (calculated using ideal Lambertian emission pattern) of 1.91 mW/cm^2 when seen from the minimum 0.1m observation distance, as specified in [16]. Hence, such a system would be theoretically eye-safe.

V. Conclusion

In this paper, we have experimentally measured an indoor optical communication channel operating at near-infrared frequency, and evaluated its frequency-domain and time-domain characteristics. Furthermore, data rate performance is measured in terms of delay spread values and eye diagrams. The eye diagrams show that there is minimal inter-symbol interference for data links operating at 800 Mbps and 1 Gbps. The immediate conclusion is that it is possible to use the optical spectrum to transmit and receive tremendous amounts of data, which has been foreseen for many years. To the author's knowledge, these are the first set of measurements attesting bit-rates as high as 1 Gbps over directed non-line-of-sight indoor optical links. It must be noted that majority of the components used in obtaining these measurements were commercial off the shelf (COTS), and hence were not specifically optimized for communication purposes. The primary intention of using these was to demonstrate the feasibility of mentioned high data rates on indoor optical wireless links. To avail of these data rates in an efficient manner, interested users must utilize custom-built or optimized optical and opto-electronic components tailored to meet the specific requirements of the data transmission system. Application of these optical links for sensor networking can significantly overcome the bandwidth and data-rate restrictions imposed on RF sensor network communications. With advances made in photonics and electronics, it is now possible to implement optical links with inexpensive low-power laser diodes and high-sensitivity wideband photo-diodes. Incorporation of these optical transmitting and receiving devices on miniaturized sensors will greatly reduce the required amount of power, and increase data rate or conversely increase number of simultaneously active links. The current analysis did not take into account the effect of interference between neighboring sensors, and optimization will be required to place and orient the sensors to reduce interference. Another problem is the loss of data due to shadowing, and an attractive and efficient way to combat shadowing and increase coverage is to use multi-spot diffuse configuration [23]. In terms of eye safety, the hypothetical data transmission systems presented in this paper would meet the requirements set out by Laser Safety standards. This is due to the diffuse nature of the laser propagation system. Further reduction of eye exposure can be achieved with the use of multiple diffusing spots on the ceiling generated by a beam-splitter. This would also benefit the communication system by providing spatial diversity. With the incorporation of a "fly-eye" receiver [4], required received power would also reduce by selectively rejecting background light. Holographic optical filters and concentrators promise

better power efficiency, as well as noise reduction [24], [25]. In general, we conclude that indoor optical wireless links have communication capabilities exceeding contemporary technologoies, and further research on system design and optimization of opto-electronic components for communication-specific applications are required for realizing the immense potentials of this emerging technology.

REFERENCES

[1] D. Kedar and S. Arnon, "Non-line-of-sight optical wireless sensor network operating in multiscattering channel," *Appl. Opt.*, vol. 45, no. 33, pp. 8454–8461, 2006.

[2] D. Kedar, E. Devila, D. Limon, and S. Arnon, , D. G. Voelz and J. C. Ricklin, Eds., *Optical Wireless Sensor Network in Multi-Scattering Channel: Laboratory Experiment*. Bellingham, WA: SPIE, 2005, vol. 5892, p. 58920Y [Online]. Available: http://link.aip.org/link/?PSI/5892/58920Y/1

[3] J. Llorca, A. Desai, U. Vishkin, C. C. Davis, and S. D. Milner, , J. D. Gonglewski and K. Stein, Eds., *Reconfigurable Optical Wireless Sensor Networks*. Bellingham, WA: SPIE, 2004, vol. 5237, pp. 136–146 [Online]. Available: http://link.aip.org/link/?PSI/5237/136/1

[4] G. Yun and M. Kavehrad, "Spot-diffusing and fly-eye receivers for indoor infrared wireless communications," in *Proc. IEEE Wireless Communications Conf. Int. Conf. Sel. Topics*, Jun. 1992, pp. 262–265.

[5] F. Gfeller and U. Bapst, "Wireless in-house data communication via diffuse infrared radiation," *Proc. IEEE*, vol. 67, no. 11, pp. 1474–1486, Nov. 1979.

[6] H. Hashemi, G. Yun, M. Kavehrad, F. Behbahani, and P. Galko, "Indoor propagation measurements at infrared frequencies for wireless local area networks applications," *IEEE Trans. Veh. Technol.*, vol. 43, no. 3, pp. 562–576, Aug. 1994.

[7] M. Pakravan, M. Kavehrad, and H. Hashemi, "Indoor wireless infrared channel characterization by measurements," *IEEE Trans. Veh. Technol.*, vol. 50, no. 4, pp. 1053–1073, Jul. 2001.

[8] Q. Jiang, M. Kavehrad, M. Pakravan, and M. Tai, "Wideband optical propagation measurement system for characterization of indoor wireless infrared channels," in *Proc. IEEE Int. Conf. Commun.* , Jun. 1995, vol. 2, pp. 1173–1176, vol. 2.

[9] J. Kahn, W. Krause, and J. Carruthers, "Experimental characterization of non-directed indoor infrared channels," *IEEE Trans. Commun.*, vol. 43, no. 234, pp. 1613–1623, Feb./Mar./Apr. 1995.

[10] J. Barry, J. Kahn, W. Krause, E. Lee, and D. Messerschmitt, "Simulation of multipath impulse response for indoor wireless optical channels," *IEEE J. Sel. Areas Commun.*, vol. 11, no. 3, pp. 367–379, Apr. 1993.

[11] C. R. Lomba, R. T. Valadas, and A. M. de Oliveira Duarte, "Efficient simulation of the impulse response of the indoor wireless optical channel," *Int. J. Commun. Syst.*, vol. 13, no. 7–8, pp. 537–549, 2000.

[12] IrDA Physical Layer Specification v1.4. Infrared Data Association. [Online]. Available: http://www.irda.org/displaycommon.cfm?an=1\&subarticlenbr=69

[13] *Wireless LAN Medium Access Control (MAC) and Physical Layer (PHY) Specifications*, IEEE Std. 802.11, 2007 [Online]. Available: http://standards.ieee.org/getieee802/802.11.html

[14] *WPAN Task Group 7 on Visible Light Communication*, IEEE 802.15 [Online]. Available: http://www.ieee802.org/15/pub/TG7.html

[15] D. C. O'Brien, S. H. Khoo, W. Zhang, G. E. Faulkner, and D. J. Edwards, E. J. Korevaar, Ed., "High-speed optical channel measurement system," in *Proc. SPIE*, Nov. 2001, vol. 4530, pp. 135–144.

[16] *Safety of Laser Products. Part 1: Equipment Classification, Requirements and User's Guide*, Std. 60 825, 2001, International Electrotechnical Commission (IEC).

[17] J. Kahn and J. Barry, "Wireless infrared communications," *Proc. IEEE*, vol. 85, no. 2, pp. 265–298, Feb. 1997.

[18] *Agilent Time Domain Analysis Using a Network Analyzer*, Agilent Technologies, application Note 1287-12. [Online]. Available: http://cp.literature.agilent.com/litweb/pdf/5989-5723EN.pdf

[19] A. V. Oppenheim, R. W. Schafer, and J. R. Buck, *Discrete-Time Signal Processing*, 2nd ed. Upper Saddle River, NJ: Prentice-Hall, Inc., 1999.

[20] A. Al-Ghamdi and J. Elmirghani, "Line strip spot-diffusing transmitter configuration for optical wireless systems influenced by background noise and multipath dispersion," *IEEE Trans. Commun.*, vol. 52, no. 1, pp. 37–45, Jan. 2004.

[21] Y. Alqudah and M. Kavehrad, "Optimum order of angle diversity with equal-gain combining receivers for broadband indoor optical wireless communications," *IEEE Trans. Veh. Technol.*, vol. 53, no. 1, pp. 94–105, Jan. 2004.

[22] J. R. Barry, *Wireless Infrared Communications*. Norwell, MA: Kluwer, 1994.

[23] M. Pakravan, E. Simova, and M. Kavehrad, "Holographic diffusers for indoor infrared communication systems," in *Proc. GLOBECOM*, Nov. 1996, vol. 3, pp. 1608–1612, vol. 3.

[24] S. T. Jivkova, S. Shurulinkov, and M. Kavehrad, "Holographic parabolic mirror as a receiver optical front end for wireless infrared communications: Experimental study," *Appl. Opt.* vol. 41, no. 28, pp. 5860–5865, 2002 [Online]. Available: http://ao.osa.org/abstract.cfm?URI=ao-41-28-5860

[25] M. Kavehrad and S. Jivkova, "Indoor broadband optical wireless communications: Optical subsystems designs and their impact on channel characteristics," *IEEE Wireless Commun.*, vol. 10, no. 2, pp. 30–35, Apr. 2003.

Jarir Fadlullah received the B.S.E.E. degree in 2004 from Bangladesh University of Engineering and Technology, Dhaka, Bangladesh. He is currently pursuing Ph.D. in electrical engineering at the Pennsylvania State University, University Park.

He is a Research Assistant at the Center for Information and Communications Technology Research (CICTR) at PSU. His research interests are multiple-input multiple-output communication system analysis, MIMO signal processing for wireless and wireline media, free-space and indoor optical channel modeling, and imaging.

Mohsen Kavehrad is with the Pennsylvania State University EE Department as Weiss Chair Professor and director of the Center for Information and Communications Technology Research. He has over 350 published papers, book chapters, books, and key patents. His research interests are in the areas of wireless and optical communications networked systems.

Dr. Kavehrad has received three Bell Labs awards, the 1990 TRIO Feedback Award for a patent on optical interconnect, the 2001 IEEE VTS Best Paper Award, three IEEE LEOS Best Paper Awards and a Canada NSERC Ph.D. thesis award with his graduate students for contributions to wireless and optical networks.